

Cannabinoid signalling inhibits sarcoplasmic Ca²⁺ release and regulates excitation–contraction coupling in mammalian skeletal muscle

Tamás Oláh¹, Dóra Bodnár¹, Adrienn Tóth¹, János Vincze¹, János Fodor¹, Barbara Reischl², Adrienn Kovács¹, Olga Ruzsnavszky¹, Beatrix Dienes¹, Péter Szentesi¹, Oliver Friedrich² and László Csernoch¹

¹Department of Physiology, Faculty of Medicine, University of Debrecen, Debrecen, Hungary

²Institute of Medical Biotechnology, Friedrich-Alexander-University Erlangen-Nürnberg, Erlangen, Germany

Key points

- Marijuana was found to cause muscle weakness, although the exact regulatory role of its receptors (CB1 cannabinoid receptor; CB1R) in the excitation–contraction coupling (ECC) of mammalian skeletal muscle remains unknown.
- We found that CB1R activation or its knockout did not affect muscle force directly, whereas its activation decreased the Ca²⁺-sensitivity of the contractile apparatus and made the muscle fibres more prone to fatigue.
- We demonstrate that CB1Rs are not connected to the inositol 1,4,5-trisphosphate pathway either in myotubes or in adult muscle fibres.
- By contrast, CB1Rs constitutively inhibit sarcoplasmic Ca²⁺ release and sarcoplasmic reticulum Ca²⁺ ATPase during ECC in a G_{i/o} protein-mediated way in adult skeletal muscle fibres but not in myotubes.
- These results help with our understanding of the physiological effects and pathological consequences of CB1R activation in skeletal muscle and may be useful in the development of new cannabinoid drugs.

Abstract Marijuana was found to cause muscle weakness, although it is unknown whether it affects the muscles directly or modulates only the motor control of the central nervous system. Although the presence of CB1 cannabinoid receptors (CB1R), which are responsible for the psychoactive effects of the drug in the brain, have recently been demonstrated in skeletal muscle, it is unclear how CB1R-mediated signalling affects the contraction and Ca²⁺ homeostasis of mammalian skeletal muscle. In the present study, we demonstrate that *in vitro* CB1R activation increased muscle fatigability and decreased the Ca²⁺-sensitivity of the contractile apparatus, whereas it did not alter the amplitude of single twitch contractions. In myotubes, CB1R agonists neither evoked, nor influenced inositol 1,4,5-trisphosphate (IP₃)-mediated Ca²⁺ transients, nor did they alter excitation–contraction coupling. By contrast, in isolated muscle fibres of wild-type mice, although CB1R agonists did not evoke IP₃-mediated Ca²⁺ transients too, they significantly reduced the amplitude of the depolarization-evoked transients in a pertussis-toxin sensitive manner, indicating a G_{i/o} protein-dependent mechanism. Concurrently, on skeletal muscle fibres isolated from CB1R-knockout animals, depolarization-evoked Ca²⁺ transients, as well as Ca²⁺ release flux via ryanodine receptors (RyRs), and the total amount of released Ca²⁺ was significantly greater than that from wild-type mice. Our results show that CB1R-mediated signalling exerts both a constitutive and an agonist-mediated inhibition on the Ca²⁺ transients via RyR, regulates the activity of the sarcoplasmic reticulum Ca²⁺ ATPase and enhances muscle fatigability, which might decrease exercise performance, thus playing a role in myopathies, and therefore should be considered during the development of new cannabinoid drugs.

(Resubmitted 26 July 2016; accepted after revision 14 September 2016; first published online 22 September 2016)

Corresponding author L. Csernoch: Department of Physiology, Faculty of Medicine, University of Debrecen, Hungary, H-4032, Debrecen, Egyetem tér 1. Email: csl@edu.unideb.hu

Abbreviations 4-CMC, 4-chloro-*m*-cresol; $[Ca^{2+}]_i$, intracellular calcium concentration; $[Ca^{2+}]_T$, total amount of calcium released; ACEA, arachidonyl-2'-chloroethylamide; AEA, anandamide (*N*-arachidonoyl ethanolamine); CaV, voltage-gated Ca^{2+} channel; CB1R, cannabinoid receptor type 1; CB2R, cannabinoid receptor type 2; DHPR, dihydropyridine receptor; ECC, excitation–contraction coupling; EDL, extensor digitorum longus; FDB, flexor digitorum brevis; FKBP12, FK-506 binding protein; IP_3 , inositol 1,4,5-trisphosphate; KO, CB1R-knockout; PKA, protein kinase A; PLB, phospholamban; PKI, PKI 14–22 amide myristoylated; PTX, pertussis toxin; PV_{max} , maximal transport rate of the Ca^{2+} pump; RyR, ryanodine receptor; SERCA, sarco/endoplasmic reticulum Ca^{2+} ATPase; SLN, sarcoplipin; Sol, soleus; SR, sarcoplasmic reticulum; STIM1, stromal interaction molecule 1; WIN, WIN55,212-2 (*R*)-(+)-[2,3-dihydro-5-methyl-3-(4-morpholinylmethyl)pyrrolo[1,2,3-*de*]-1,4-benzoxazin-6-yl]-1-naphthalenylmethanone mesylate; WT, wild-type.

Introduction

The receptors of the psychoactive compound of marijuana can also be activated by endogenous ligands, such as anandamide (Devane *et al.* 1992) and 2-arachidonoyl glycerol. These ligands are produced, detected and degraded by the endocannabinoid system (Pertwee *et al.* 2010). The main cannabinoid receptor (CB1 receptor; CB1R) is present both in neural and peripheral tissues (Pertwee *et al.* 2010; Maccarrone *et al.* 2015) and can connect to different G proteins ($G_{i/o}$, G_q and G_s), depending on the cell type (Lauckner *et al.* 2005; Turu and Hunyady 2010). This ubiquity and versatility enables a wide variety of regulatory functions (e.g. motor co-ordination, memory, appetite, pain modulation, neuroprotection, cognitive functions, affective states and maintenance of energy homeostasis) (Fišar *et al.* 2014). Inhibition of the endocannabinoid system by neutral CB1R antagonists in the peripheral organs is one of the most promising ways of treating obesity, whereas the activation of CB1Rs (e.g. medical marijuana) in the nervous system can be used to treat nausea, vomiting, anorexia, weight loss, muscle spasms and pain (Borgelt *et al.* 2013; Pacher and Kunos 2013). Thus, in the organs responsible for these effects, the role of CB1Rs has been studied extensively. However, there are organs in which the physiological role of the cannabinoid system is much less understood.

The skeletal muscle system comprises 30–40% of the body mass in humans. It is responsible for all the voluntary movements and it is also a key player in glucose metabolism (Sinacore and Gulve 1993) and thermoregulation (Rowland *et al.* 2015) of the body. The expression of CB1 and CB2 cannabinoid receptors and the enzymes responsible for the synthesis (*N*-acyl phosphatidylethanolamine-selective phospholipase D, diacylglycerol lipase α and β) and degradation (fatty acid amide hydrolase, monoacylglycerol lipase) of the endocannabinoid compounds has recently been demonstrated in mammalian skeletal muscle (Cavuto *et al.* 2007; Crespillo *et al.* 2011; Hutchins-Wiese *et al.*

2012). To date, the role of cannabinoid signalling in glucose uptake and energy balance of the muscle has been well described: inhibition of CB1R decreases insulin resistance (Taube *et al.* 2009), augments glucose uptake (Lindborg *et al.* 2010) and decreases body weight (Crespillo *et al.* 2011) in a protein kinase A (PKA)-dependent way by stimulating the expression and activity of phosphatidylinositol-3-kinase (Esposito *et al.* 2008) and extracellular signal-regulated kinase 1/2 (Lipina *et al.* 2010). In myogenesis, CB1R activation was also shown to decrease myoblast differentiation via inhibition of Kv7.4 channels (Iannotti *et al.* 2014).

However, surprisingly, in the regulation of the main and most obvious function of skeletal muscle (i.e. contraction), the exact role of the cannabinoid system still awaits clarification. Cannabinoids were found to affect muscle activity, although whether they acted on the muscles directly, or affected them indirectly, solely by modulating their nervous control was not investigated. In these studies, smoking marijuana caused muscle weakness (Lorente Fernandez *et al.* 2014) and muscle fatigue (Renaud and Cormier 1986) in human patients, and activation of CB1Rs decreased (and their inhibition increased) the locomotor activity of treated mice (Zimmer *et al.* 1999). To our knowledge, only one study has unequivocally shown that the tested cannabinoids acted directly on the muscles, although this study was performed on frog muscles, and its transferability to human physiology is limited. In that study, CB1R agonists attenuated the caffeine-induced force transients (Huerta *et al.* 2009). Thus, there is a need for related results on clinically more relevant mammalian experimental models. Moreover, if cannabinoids directly altered contractile force or fatigue of mammalian muscles, this would indicate an as yet uninvestigated adverse effect or even a new target for cannabinoid drug development. Furthermore, because there is an unexpectedly high rate (>25%) of marijuana use among student athletes (Buckman *et al.* 2011), knowing how marijuana smoking affects exercise performance could be a strong argument for the future success of drug prevention.

If the fatigue and weakness described above originated directly in the muscle, it might be hypothesized that CB1R activation regulates excitation–contraction coupling (ECC) by a yet unknown mechanism. ECC is a process during which the depolarization of the plasma membrane activates dihydropyridine receptors (DHPR) that mechanically couple to ryanodine receptors (RyR) to release Ca^{2+} from the sarcoplasmic reticulum (SR) as required for muscle contraction (Franzini-Armstrong and Protasi 1997). To enable muscle relaxation, Ca^{2+} is subsequently re-uptaken by the sarco/endoplasmic reticulum Ca^{2+} ATPase (SERCA) (Stammers *et al.* 2015). However, the ECC step affected by the CB1R-mediated signalling remains unclear. In skeletal muscle, even the immediate downstream signalling partners of CB1Rs are highly debated. In some cell types, CB1R is connected to G_q proteins and the inositol 1,4,5-trisphosphate (IP_3) pathway, causing an elevation of intracellular calcium concentration ($[\text{Ca}^{2+}]_i$) (Lauckner *et al.* 2005; Navarrete and Araque 2008) and the same mechanism was proposed for skeletal myoblast cell cultures in a recent study (Iannotti *et al.* 2014). By contrast, in another study, the effects of CB1R activation in frog skeletal muscle were assumed to be mediated in a $G_{i/o}$ protein-dependent way (Huerta *et al.* 2009), similar to the majority of other studies performed on various non-muscle cell types (Turu and Hunyady 2010). The exact steps of the signalling cascade by which CB1Rs affect muscle force and Ca^{2+} homeostasis in adult mammalian skeletal muscle fibres also remain to be discovered.

In the present study, we aimed to decipher the signalling pathways and to understand the role played by CB1Rs in muscle performance, contractions and Ca^{2+} homeostasis using a CB1R-knockout (KO) animal model, applying *in vivo* muscle performance tests, *in vitro* force measurements, single-cell Ca^{2+} imaging, confocal microscopy and biochemical techniques. The results obtained indicate that CB1Rs localize around the Z-lines, and constitutively inhibit SR Ca^{2+} release during ECC in a $G_{i/o}$ protein-mediated way in adult skeletal muscle fibres but not in myotubes. Moreover, CB1R activation decreases the Ca^{2+} sensitivity of the contractile proteins and increases muscle fatigue.

Methods

Ethical approval, animal care and KO mice

Animal experiments conformed with the guidelines of the European Community (86/609/EEC) and the institutional Animal Care Committee of University of Debrecen (31/2012/DE MAB). KO mice were a kind gift from Dr Andreas Zimmer (Zimmer *et al.* 1999). Eight- to 10-week-old wild-type C57BL/6 (WT) and KO mice were used for the experiments. The mice were housed in

plastic cages with mesh covers, and fed with pelleted mouse chow and water *ad libitum*. Room illumination comprised an automated 12:12 h light/dark cycle, and room temperature was maintained within the range 22–25°C. When necessary, mice were killed by cervical dislocation after anaesthesia with pentobarbital.

In vivo muscle performance measurements

Voluntary activity wheel measurements, forepaw grip tests and wire hang tests were performed as described previously (Oddoux *et al.* 2009, Bodnár *et al.* 2014).

Measurement of muscle force and fatigability on whole muscles

Muscle contractions of fast extensor digitorum longus (EDL) and slow soleus (Sol) muscles were measured as described previously (Oddoux *et al.* 2009). A series of single electric pulses (5 V), 2 or 4 s apart, was used to elicit single twitches in EDL and Sol muscles, respectively. To elicit a tetanus, single pulses were applied with a frequency of 100 Hz for 200 ms in the case of EDL and 50 Hz for 500 ms in the case of Sol. Series of tetani were recorded with a frequency of 0.25 trains s^{-1} . In a series of stimulation, at least 10 twitches or tetani were measured under these conditions from every muscle; and two consecutive series were compared on each muscle. Between two following series, 5 min of intermittent period was applied for relaxation and recovery of the muscles and for treatment with the CB1R agonist 1 μM WIN55,212-2 (*R*)-(+)-[2,3-dihydro-5-methyl-3-(4-morpholinylmethyl)pyrrolo[1,2,3-*de*]-1,4-benzoxazin-6-yl]-1-naphthalenylmethanone mesylate (WIN) (Tocris Bioscience, Bristol, UK), both for twitches and tetani.

To test muscle fatigability, 150 tetanic contractions (200 Hz for 200 ms) at a frequency of 0.5 Hz were evoked (Oddoux *et al.* 2009). The amplitude of each tetanus was normalized to that of the largest in the series (usually the first or the second) and plotted as a function of the position within the series. In some experiments, WT muscles were pre-treated with 1 μM WIN for 1 h before and during the measurement.

Measurement of muscle force in small fibre bundles

Small fibre bundles of five fibres were mechanically isolated from EDL muscles of WT mice. The ends of the bundles were cut, which enabled a moderate exchange between the intra- and extracellular solutions. A computer-aided force transducer system based on a KG-7 sensor (MyoTronik, Heidelberg, Germany) (similar to that reported in Friedrich *et al.* 2014) was used to measure isometric contractions of the bundles. Contractions were evoked by dipping the bundles into different solutions

using a custom designed, motorized, programmable rack of wells. Experiments were performed at 30°C. During the measurements, the solutions used were: (i) high activating solution containing 30 mM caffeine and the maximal physiologically active $[Ca^{2+}]$ for evoking contractures, containing (in mM): 30 Hepes, 6.05 Mg(OH)₂, 30 EGTA, 29 CaCO₃, 8 Na₂ATP, 10 Na₂-creatine phosphate and 1% creatine kinase; (ii) high relaxing solution for washout of Ca²⁺ after every Ca²⁺-containing solutions and to induce relaxation, containing (in mM): 30 Hepes, 6.25 Mg(OH)₂, 30 EGTA, 8 Na₂ATP, 10 Na₂-creatine phosphate and 1% creatine kinase; and (iii) low relaxing solution for washout of high EGTA prior to release, baseline recording and treatment with 1 μM WIN, containing (in mM): 30 Hepes, 7.86 Mg(OH)₂, 87.7 K-glutamate, 0.4 EGTA, 6.6 HDTA, 8 Na₂ATP, 10 Na₂-creatine phosphate and 1% creatine kinase.

Ca²⁺ sensitivity of the contractile apparatus

EDL fibre bundles of WT mice were either untreated or treated with 1 μM WIN for 15 min and then chemically skinned with 0.1% saponin for 2 min. Ca²⁺ contractures were evoked by immersing the bundles from a highly-buffered EGTA containing Ca²⁺-free 'high relaxing solution' to activating solutions (high relaxing solution supplemented with Ca²⁺) of gradually increasing $[Ca^{2+}]$. Isometric force values were normalized for the maximal Ca²⁺-activated active force, and Ca²⁺-force relationships were plotted to determine the Ca²⁺-sensitivity of isometric force production. The relationship between force and pCa was fitted with a Hill equation; with the Hill coefficient being a measure of the co-ordinativity and pCa₅₀ reflecting the Ca²⁺-sensitivity.

Cell cultures

C2C12 cells were cultured using a standard protocol described previously (Oláh *et al.* 2011). Functional experiments were carried out on 5–6-day-old terminally differentiated myotubes.

Isolation of single skeletal muscle fibres

Experiments were carried out on fibres from the flexor digitorum brevis (FDB) muscles of the mice. Single muscle fibres were enzymatically dissociated in calcium free modified Tyrode solution (in mM: 137 NaCl, 5.4 KCl, 0.5 MgCl₂ and 11.8 Hepes, pH 7.4; all from Sigma, St Louis, MO, USA) containing 0.2% Type I collagenase (Sigma) at 37°C for 50–55 min (Bodnár *et al.* 2014) and were then stored in a refrigerator until further use. To release single fibres, muscles were triturated gently in normal Tyrode solution (in mM: 137 NaCl, 5.4 KCl, 0.5 MgCl₂, 1.8 CaCl₂, 11.8 Hepes and 1 g l⁻¹ glucose, pH 7.4; all from

Sigma) containing 1.8 mM CaCl₂. The fibres were then mounted on laminin-coated coverslips and used for the experiments.

Immunocytochemistry

FDB fibres were fixed with 2% paraformaldehyde in 50% methanol for 15 min, permeabilized with 0.5% Triton X-100 in PBS for 10 min, and blocked with 0.2% Triton X-100 diluted in Serum-Free Protein Block (Dako, Glostrup, Denmark) for 30 min at room temperature. The cells were then incubated overnight at 4°C with primary antibodies diluted in Serum-Free Protein Block: CB1R (dilution 1:50, SC-20754; Santa Cruz Biotechnology, Heidelberg, Germany), RyR (dilution 1:500, MA3-925; Thermo Fisher Scientific, Waltham, MA, USA), α-actinin (dilution 1:50, SC-7453; Santa Cruz Biotechnology). Then, Cy3 (dilution 1:800, A-10520; Thermo Fisher Scientific), Alexa Fluor 488 (dilution 1:800, A-11001; Thermo Fisher Scientific) and Dylight 488 (dilution 1:800, DI-3088; Vector Laboratories, Burlingame, CA, USA) labelled secondary antibodies were applied for 1 h at room temperature. Vectashield mounting medium with DAPI (Vector Laboratories) was used to make the nuclei visible. Images were taken using a laser scanning microscope system (LSM 510 META confocal microscope; Zeiss, Oberkochen, Germany) with a Plan-Neofluar 40×/1.3 Oil DIC objective (Zeiss). For statistical analysis of the images, Imaris scientific image processing and analysing software (Bitplane, Zurich, Switzerland) was applied.

Single-cell calcium imaging

Changes in $[Ca^{2+}]_i$ of C2C12 myotubes and isolated FDB fibres were measured using the calcium sensitive fluorescent dye Fura-2 as reported previously (Oláh *et al.* 2011). Cells were continuously washed with normal Tyrode solution using a background perfusion system. Test solutions were directly applied to the cells through a perfusion capillary tube (Perfusion Pencil™; Auto-Mate Scientific, San Francisco, CA, USA) with an internal diameter of 250 μm at a rate of 0.35 ml min⁻¹, using a local perfusion system (Valve Bank™ 8, version 2.0; Auto-Mate Scientific). The excitation wavelength was alternated between 340 and 380 nm using a dual wavelength monochromator (Deltascan, Photon Technology International, New Brunswick, NJ, USA), whereas emission was monitored at 510 nm using an interference filter and a photomultiplier. $[Ca^{2+}]_i$ was calculated from the ratio of fluorescence intensities ($R = F_{340}/F_{380}$) using an *in situ* calibration (Oláh *et al.* 2011). Ca²⁺ binding to intracellular binding sites and the removal of Ca²⁺ from the intracellular space were modelled as described in earlier studies (Szappanos *et al.* 2004; Oláh *et al.* 2011) to determine the

activity of the Ca^{2+} pump and the Ca^{2+} flux entering the myoplasmic space.

The CB1R agonists WIN, arachidonyl-2'-chloroethylamide (ACEA; Cayman Chemical, Tallinn, Estonia) and anandamide (AEA) (Tocris Bioscience) were used at a final concentration of 1 or 10 μM in normal Tyrode solution. KCl was applied at a final concentration of 120 mM in normal Tyrode solution by replacing an equal amount of NaCl. ATP was used at a final concentration of 180 μM . 4-chloro-*m*-cresol (4-CMC), the direct activator of RyR was used at a concentration of 2 mM. When FDB fibres were measured, 50 μM *N*-benzyl-*p*-toluenesulfonamide (Tocris Bioscience) was added to the solutions to prevent the contraction of fibres. Pertussis toxin (PTX; from Sigma) was used at a concentration of 1 $\mu\text{g ml}^{-1}$ as an overnight pre-treatment in some experiments.

Western blot analysis

Whole hind limb muscle homogenates of at least 3 WT and 3 KO mice were collected separately and Western blot analysis was performed as described previously (Oláh *et al.* 2011). The antibodies used were: SERCA1 (dilution 1:1000; a kind gift from E. Zádor), RyR1 (dilution 1:1000, MA3-925; Thermo Fisher Scientific), DHPR (dilution 1:500, MA3-921; Thermo Fisher Scientific), FK-506 binding protein (FKBP12) (dilution 1:200, sc-6174; Santa Cruz Biotechnology), calsequestrin (dilution 1:1000, PA1-913; Thermo Fisher Scientific), stromal interaction molecule 1 (STIM1) (dilution 1:500, 610954; BD Biosciences, Franklin Lakes, NJ, USA), Orai1 (dilution 1:500, MA5-1577; Thermo Fisher Scientific), cannabinoid receptor type 2 (CB2R) (dilution 1:1000, AB45942; Abcam, Cambridge, UK), PKA (dilution 1:100, sc-365615; Santa Cruz Biotechnology) and actin (dilution 1:200, sc-1616 and sc-1616-R; Santa Cruz Biotechnology). As secondary antibodies, horseradish peroxidase conjugated goat anti-mouse and goat anti-rabbit IgGs (dilution 1:1000; Bio-Rad, Hercules, CA, USA) were employed and the immunoreactive bands were visualized using a SuperSignal West Pico or Femto Chemiluminescent Substrate-Enhanced Chemiluminescence kit (Thermo Fisher Scientific) in conjunction with a Gel Logic 1500 Imaging System (Kodak, Tokyo, Japan). Densitometric analysis was performed with ImageJ (NIH, Bethesda, MD, USA). The optical density of the bands was normalized to actin of the same sample, and then to WT.

Detection of the changes in $[\text{Ca}^{2+}]_i$ using confocal microscopy

Confocal measurements were performed as described previously (Bodnár *et al.* 2014). To mimic the conditions used for the force measurements, individual action

potentials and tetanic depolarizations were initiated by field-stimulation using supra-threshold single 2 ms long square pulses or trains of 2 ms long square pulses with a frequency of 50 Hz within the train. Each train lasted for 100 ms. Depolarization-evoked calcium transients were measured using a confocal laser scanning microscope system (LSM 5 Live and LSM 510 Meta; Zeiss) after loading the fibres with 20 μM Rhod-2 AM or Fluo-8-AM (Biotium, Inc., Hayward, CA, USA) for 30 min at room temperature. Line-scan images (512 pixels/line) were used to monitor the fluorescence intensity changes at 0.5 or 1.93 ms line^{-1} with a 20x/0.5 objective. To obtain the time-course of Rhod-2 fluorescence change, corresponding data points (usually 10–15) in the line-scan images were averaged in the spatial domain. Resting fluorescence was determined as the average fluorescence before depolarization. Changes in $[\text{Ca}^{2+}]_i$, the released amount of Ca^{2+} ($[\text{Ca}^{2+}]_T$) and the calcium release flux were calculated as described previously (Bodnár *et al.* 2014). Finally, 1 μM PKI 14–22 amide myristoylated (PKI) (Tocris Bioscience), the inhibitor of PKA, and 20 μM gallein (Tocris Bioscience), the inhibitor of the $G\beta\gamma$ subunit, were used as 5 min long treatments between two consecutive single stimulatory impulse-evoked Ca^{2+} transients. The drugs were dissolved in DMSO, and DMSO alone was used as a vehicle control.

Statistical analysis

Data are presented as the mean \pm SEM (n , number of observations). Normality of the data was tested with the Shapiro–Wilk test. In paired experiments, Student's paired t test or the Wilcoxon signed rank test was used to determine significant differences depending on the normality of the data. When two, non-paired groups were compared, Student's t test or the Mann-Whitney rank sum test was applied. When multiple groups were compared, one-way ANOVA or Kruskal–Wallis one-way ANOVA on ranks was used to determine significant differences between the groups, followed by Holm–Sidak's or Dunn's multiple comparisons test, respectively. In all tests, $P < 0.05$ was considered statistically significant. Analyses were performed with SigmaPlot, version 12.0 (Systat Software, Inc., San Jose, CA, USA) and Prism, version 6 (GraphPad Software, Inc., La Jolla, CA, USA).

Results

CB1 receptors are localized around the Z-lines of adult muscle fibres

Expression of CB1R has been reported in skeletal muscle (Cavuto *et al.* 2007; Crespillo *et al.* 2011); however, its subcellular localization has not yet been investigated. In the present study, enzymatically isolated FDB fibres from

WT mice were co-immunolabelled with antibodies against CB1R and RyR (Fig. 1A–F) and fluorescence intensities of the images (Fig. 1D–F) were plotted to examine the overlap of red and green signals (Fig. 1G–I). RyR showed a typical double-band labelling, corresponding to the localization of two T-tubules in each sarcomere. CB1R showed a striated pattern between the double bands corresponding to the RyR, indicating its localization in the I-band, around the Z-line. The ratio of the co-localizing pixels was $12.4 \pm 2.5\%$ ($n = 11$).

To define the localization of CB1Rs more accurately, CB1R and α -actinin were co-immunolabelled (Fig. 1G–I) and fluorescence intensities of the images were plotted (Fig. 1J–L). The peaks of the fluorescence intensity curves clearly overlapped (Fig. 1L), confirming the co-localization of the two proteins at the Z-line. The ratio of the co-localizing pixels was $60.7 \pm 10.7\%$ ($n = 6$), which was significantly higher ($P < 0.005$) compared to

that of CB1R and RyR. Pearson's correlation coefficients were also determined, with values of 0.065 ± 0.016 for CB1R and RyR and 0.370 ± 0.047 for CB1R and α -actinin.

In vivo and *in vitro* muscle force and fatigability are altered in CB1R KO and CB1R agonist-treated muscles

To examine the effects of CB1 receptor deficiency on *in vivo* muscle performance, activity-wheel tests (Fig. 2A–C), wire hang tests (Fig. 2D) and forepaw grip tests (Fig. 2E) were performed, with CB1R KO (KO) mice performing significantly worse ($P < 0.01$) compared to WT. These differences may indicate a deficiency (i) of primary muscular origin or (ii) on the nervous system side. To address the former option in more detail, *in vitro* force measurements were performed.

A series of twitch or tetanic electrical stimulation was applied to isolated EDL (Fig. 3) and Sol muscles, and

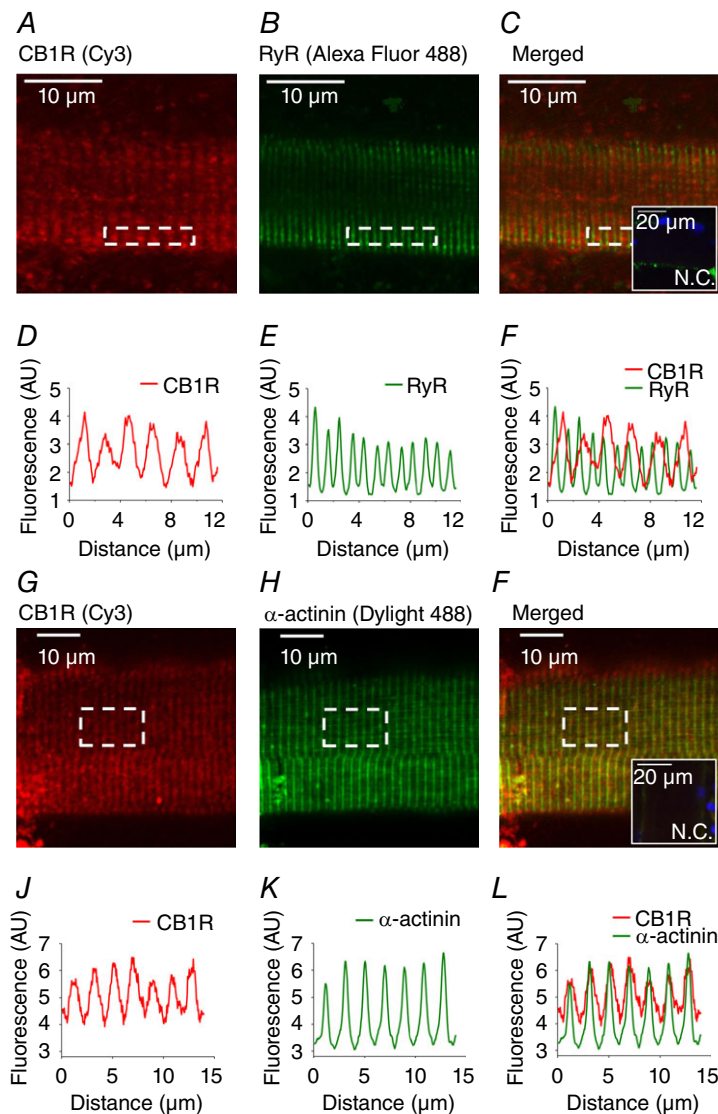


Figure 1. CB1 receptor localizes around the Z-lines of FDB fibres

Representative confocal immunofluorescence images showing the localization of (A and G) CB1R (labelled with Cy3, red) around the Z-lines, (B) ryanodine receptors (RyR, labelled with Alexa Fluor 488, green) in the T-tubules of the SR and (H) α -actinin at the Z-lines (labelled with Dylight 488, green). C and I, merged images of (A) and (B) with (G) and (H), respectively. C and I, inset: a negative control image, stained with both secondary antibodies and showing labelling of the nuclei (DAPI, blue). D–F and J–L, fluorescence intensity of (A) to (C) and (G) to (I), respectively, plotted under each image. Images were recorded from 1 μ m thick optical slices. Original magnification: 40 \times .

force was recorded in the absence or presence of the CB1R agonist WIN (1 μ M). Neither twitch (Fig. 3A, B and E), nor tetanic (Fig. 3C, D and F) muscle force of KO mice differed ($P > 0.05$) from WT. WIN appeared to be ineffective both in short series of contractions of whole muscles (Fig. 3E–F), and also in small EDL fibre bundles (data not shown) but, interestingly, 1 h of treatment of the WT muscles with 1 μ M WIN significantly ($P < 0.05$) increased fatigability (Fig. 3G). Similarly to EDL, we did not observe any significant differences for whole Sol muscles in the force either between WT and KO, or in the absence and presence of WIN (data not shown). Furthermore, 1 h of pre-treatment of WT Sol muscles with 1 μ M WIN significantly ($P < 0.05$) increased fatigability (data not shown).

To examine the possibility that these changes were a result of alterations in the calcium sensitivity of the contractile proteins, pCa–force relationships were assessed in untreated and 1 μ M WIN-pre-treated and then permeabilized WT fibre bundles (Fig. 3H). The normalized pCa–force relationships were fitted with a Hill equation (Fig. 3I). The Hill coefficient did not change ($P = 0.15$), although the pCa₅₀ value was lower ($P < 0.05$) in the WIN-treated fibre bundles (Fig. 3J), indicating that the Ca²⁺ sensitivity of the contractile apparatus significantly decreased when CB1Rs were activated. That is, in WIN-treated fibre bundles, a higher elevation of [Ca²⁺]_i is needed (6.7 \pm 0.5 μ M vs. 5.2 \pm 0.4 μ M in pre-treated vs. untreated, respectively) to achieve the half-maximal activation of the contractile apparatus.

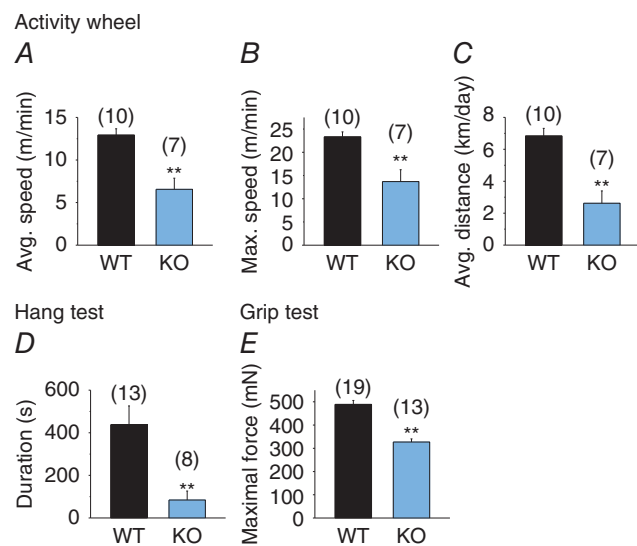


Figure 2. In vivo muscle performance of KO and WT mice
Average speed (A), maximum speed (B) and average distance per day (C) measured with voluntary activity-wheel test. D, average duration, measured with wire hang tests. E, average maximal force of the animals measured with grip tests. ** $P < 0.01$, WT vs. KO mice. [Colour figure can be viewed at wileyonlinelibrary.com]

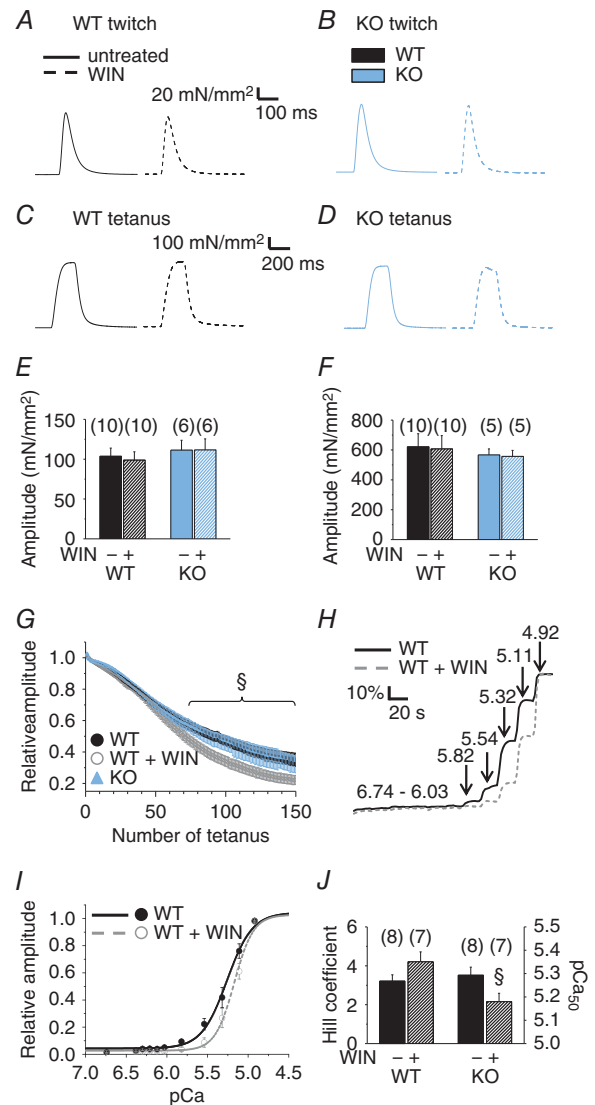


Figure 3. CB1R activation enhances fatigue and attenuates Ca²⁺ sensitivity
To evoke contractions, repeated series of electrical stimulation were applied to isolated whole EDL muscles in the absence and presence of the CB1R agonist 1 μ M WIN, and force was measured. Representative single twitches (A and B) and tetani (C and D) of WT (A and C) and KO EDL muscle (B and D) are shown. A continuous line indicates a representative contraction in the absence, whereas a dashed line indicates one in the presence of WIN. Pooled data of the amplitudes of (E) single twitches and (F) tetani in the absence and presence of WIN. Numbers in parentheses show the number of muscles studied. G, time course of the amplitude of tetani in EDL muscles. Altogether, 150 tetani, repeated every 2 s, were evoked, and their amplitudes normalized to the maximum train value. Measurements were pooled from six KO, six WT and five WIN-treated (1 μ M for 1 h) WT EDL muscles. § $P < 0.05$, WIN-treated vs. untreated muscles. H, representative pCa–relative force curves of an untreated and a 1 μ M WIN-pre-treated WT EDL fibre bundle. Numbers on arrows indicate the pCa steps. I, Hill-fit of the pCa–force values normalized to the maximal force. J, pooled data of Hill coefficients and pCa₅₀ values. n, number of fibre bundles. § $P < 0.05$, WIN-treated vs. untreated fibre bundles. [Colour figure can be viewed at wileyonlinelibrary.com]

CB1R agonists do not evoke Ca²⁺ transients via the IP₃ pathway in myotubes and adult muscle fibres

To examine the direct effects of CB1R agonists on the Ca²⁺ homeostasis of skeletal muscle cells in different developmental stages, 1 μM ACEA and 1 μM WIN were administered to Fura-2-loaded terminally differentiated C2C12 myotubes (*n* = 51) (Fig. 4A) and FDB muscle fibres from WT mice (*n* = 53) (Fig. 4B). None of these agonists was able to evoke a Ca²⁺ transient, in contrast to the 120 mM KCl and 180 μM ATP used as viability controls. To examine the possibility that peripheral CB1 receptors have a lower affinity for the aforementioned agonists, ACEA and WIN were applied in a 10 μM concentration on WT FDB fibres (Fig. 4C), although none of the tested fibres (*n* = 13) responded to these agonists with a Ca²⁺ transient in contrast to the 120 mM KCl.

In C2C12 myotubes, the regulatory effects of CB1Rs on the IP₃-mediated Ca²⁺ release were also tested. The IP₃ pathway was activated by 180 μM ATP in Ca²⁺-free solution (i.e. to activate only the P2Y metabotropic without the effects of Ca²⁺ entry via P2X ionotropic purinergic receptors; Burnstock *et al.* 2013) in the absence (Fig. 4D) and presence (Fig. 4E) of the CB1R agonist 1 μM WIN. The amplitude of the ATP-evoked Ca²⁺ transients did not differ significantly (*P* = 0.76) between untreated and WIN-treated myotubes (Fig. 4F).

These observations strongly suggest that CB1 receptors are not coupled functionally to G_q proteins and the IP₃ pathway in skeletal muscle.

In developing muscle, the CB1R agonist WIN has no effect on Ca²⁺ transients

To determine the functionality of CB1 receptors in developing muscle, the effects of the CB1R agonist 1 μM WIN was tested on the KCl depolarization-evoked

Ca²⁺ transients of terminally differentiated C2C12 myotubes loaded with Fura-2 (Fig. 5). Both in the absence (Fig. 5A) and presence of WIN (Fig. 5B), the amplitude of the second transient evoked by KCl-depolarization was marginally lower, although statistically significant (*P* < 0.05) compared to the first one (Fig. 5C). The presence of WIN did not alter (*P* = 0.55) the amplitude of the second transients compared to the untreated ones. Furthermore, the relationship between the amplitudes of the second and first transients (expressed as a percentage of the first transient) was unchanged in the presence of WIN (92 ± 3%, *n* = 14 in untreated *vs.* 91 ± 3%, *n* = 15 in WIN-treated cells; *P* = 0.72) (Fig. 5D). These results indicate that CB1 receptors have no effect on the DHPR-RyR-mediated Ca²⁺ release on cells in the myotube stage of muscle development.

Depolarization-evoked Ca²⁺ transients are augmented in KO fibres and can be attenuated by the CB1R agonist WIN and AEA in WT fibres

To explore the function of CB1 receptors in the regulation of depolarization-evoked Ca²⁺ transients in adult muscle, FDB fibres were enzymatically isolated from WT and KO mice. Ca²⁺ release in Fura-2 loaded fibres was activated by repeated application of 120 mM KCl (Fig. 6A and B). The amplitude of the first Ca²⁺ transients was significantly (*P* < 0.01) higher in KO fibres compared to WT (Fig. 6G). Our observation that the ablation of CB1 receptors causes an increase in the depolarization-evoked Ca²⁺ transients suggests a constitutive CB1R activity (Nie and Lewis 2001) and a sustained negative regulatory role of these receptors on ECC that was abolished in the KO animals.

To examine this hypothesis, the effect of 1 μM WIN was studied on KCl-evoked Ca²⁺ transients (Fig. 6C and D). Two transients were evoked; the only difference was

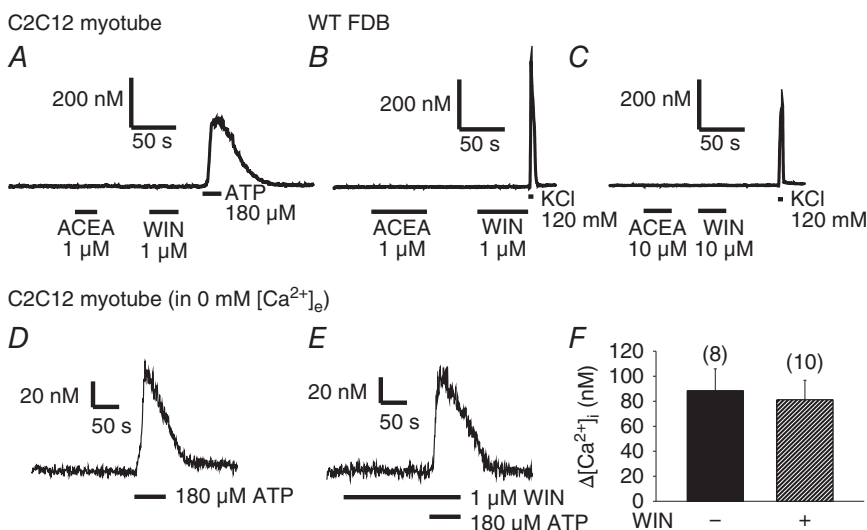


Figure 4. CB1R agonists do not evoke Ca²⁺ transients via the IP₃ pathway in myotubes and adult muscle fibres
Representative traces of single-cell [Ca²⁺]_i measurements performed on Fura-2-loaded (A) C2C12 myotubes (*n* = 51) and (B) FDB fibres of WT mice (*n* = 53). The CB1R agonists 1 μM ACEA and 1 μM WIN did not evoke Ca²⁺ transients as opposed to 120 mM KCl or 180 μM ATP used as viability controls. Even when applied at 10 μM (C), these agonists could not evoke Ca²⁺ transients as opposed to KCl in FDB fibres (*n* = 13). However, the IP₃ pathway was clearly activated in C2C12 myotubes by the administration of 180 μM ATP in Ca²⁺-free Tyrode solution in the (D) absence and (E) presence of 1 μM WIN. F, pooled data of the amplitude of the ATP-evoked transients.

the absence or presence of WIN after the first transients. Although the presence of WIN significantly ($P < 0.01$) reduced the amplitude of the second KCl-evoked transients in WT fibres, it had no such effect in KO fibres (Fig. 6H). In addition, the effect of WIN in WT fibres was greatly occluded by an overnight treatment with $1 \mu\text{g ml}^{-1}$ PTX (Fig. 6E and H), an inhibitor of $G_{i/o}$ proteins. A similar effect was not observable in PTX-treated KO fibres (Fig. 6F and H).

To further quantify these results and to enable the comparison between the different groups, the ratio of the amplitudes of the transients was calculated. The ratio is obtained by dividing the amplitude of the second transient by that of the first of the same fibre. This ratio decreased significantly in WT fibres upon WIN treatment ($72 \pm 5\%$, $n = 25$ in untreated vs. $44 \pm 7\%$, $n = 27$ in WIN-treated fibres; $P < 0.01$) (Fig. 6H) but was similar to the untreated ones in KO fibres ($61 \pm 4\%$, $n = 47$ in untreated vs. $61 \pm 5\%$, $n = 27$ in WIN-treated fibres; $P = 0.98$) (Fig. 6H). This indicates that WIN not only attenuated the amplitude of the Ca^{2+} transients in WT fibres, but also that this effect was specific for CB1Rs. Moreover, PTX treatment in WT fibres reversed the effect of WIN on this ratio to a value similar to that observed in KO fibres ($63 \pm 7\%$, $n = 18$; $P > 0.05$) (Fig. 6H) but was ineffective in KO fibres ($62 \pm 7\%$, $n = 8$).

Because WIN is a synthetic agonist of the cannabinoid receptors, the effects of the endogenous CB1R agonist AEA were also tested on WT FDB fibres. The presence

of AEA significantly ($P < 0.01$) reduced the amplitude of the second KCl-evoked transients. The ratio of the second transient of each cell compared to their first transient was smaller in AEA-treated ($49 \pm 6\%$, $n = 14$) than in untreated ($72 \pm 5\%$, $n = 25$) fibres ($P < 0.01$) (Fig. 6H). These results strengthen the previous observations that CB1 receptors negatively regulate the depolarization-evoked Ca^{2+} release.

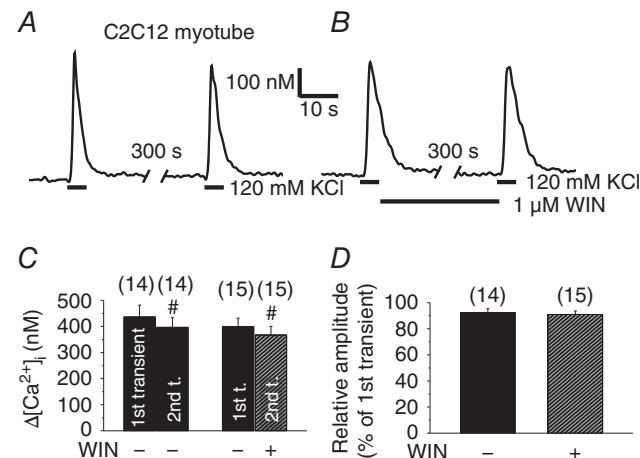


Figure 5. CB1R activation has no effect on the Ca^{2+} transients in myotubes
 Representative records showing repeated KCl-depolarization-evoked Ca^{2+} transients of Fura-2 loaded, terminally differentiated C2C12 myotubes. The cannabinoid agonist WIN ($1 \mu\text{M}$) was (A) absent or (B) present in the media after the first transient. Pooled data of the amplitude of the transients (C) and the relationship between the amplitudes (D) of the first and second transients expressed as a percentage of the first transient. # $P < 0.05$, first vs. second transient of the same cell.

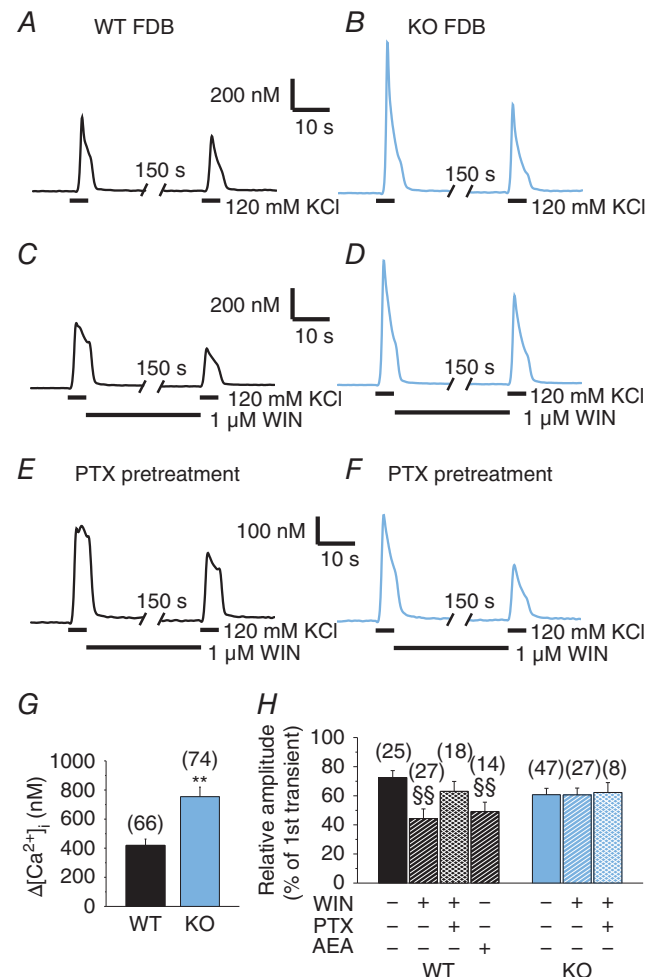


Figure 6. CB1R activation attenuates; its absence enhances the Ca^{2+} transients in adult FDB fibres via a $G_{i/o}$ -mediated way
 Repeated KCl-depolarization-evoked Ca^{2+} transients of Fura-2 loaded FDB muscle fibres from KO and WT mice in the absence and presence of CB1R agonists. Representative records of (A) WT and (B) KO FDB fibres in the absence of WIN ($1 \mu\text{M}$). Representative records of (C) WT and (D) KO FDB fibres in the presence of WIN. WIN was continuously applied after the first transients. Representative records of (E) WT and (F) KO FDB fibres pre-treated with $1 \mu\text{g ml}^{-1}$ PTX (a $G_{i/o}$ protein inhibitor) overnight before measurement. G, pooled data of the amplitude of the first transients without PTX. H, relationship between the amplitudes of the first and second transients expressed as a percentage of the first transient. * $P < 0.05$ and ** $P < 0.01$, respectively, WT vs. KO mice. ### $P < 0.01$, first vs. second transient of the same fibre. §§ $P < 0.01$, WIN- or AEA-treated vs. untreated fibres. [Colour figure can be viewed at wileyonlinelibrary.com]

SERCA activity and expression are reduced, while the Ca^{2+} flux via RyRs is increased in KO fibres

The maximal transport rate of the SERCA pump (PV_{max}) was determined from the declining phase of the Ca^{2+}

transients following the KCl-depolarization (Szappanos *et al.* 2004; Oláh *et al.* 2011). In KO FDB fibres, PV_{max} was not significantly different ($P = 0.06$) from WT. In WT, but not in KO, it increased significantly after PTX treatment ($P < 0.01$) (Fig. 7A). By contrast, WIN treatment did

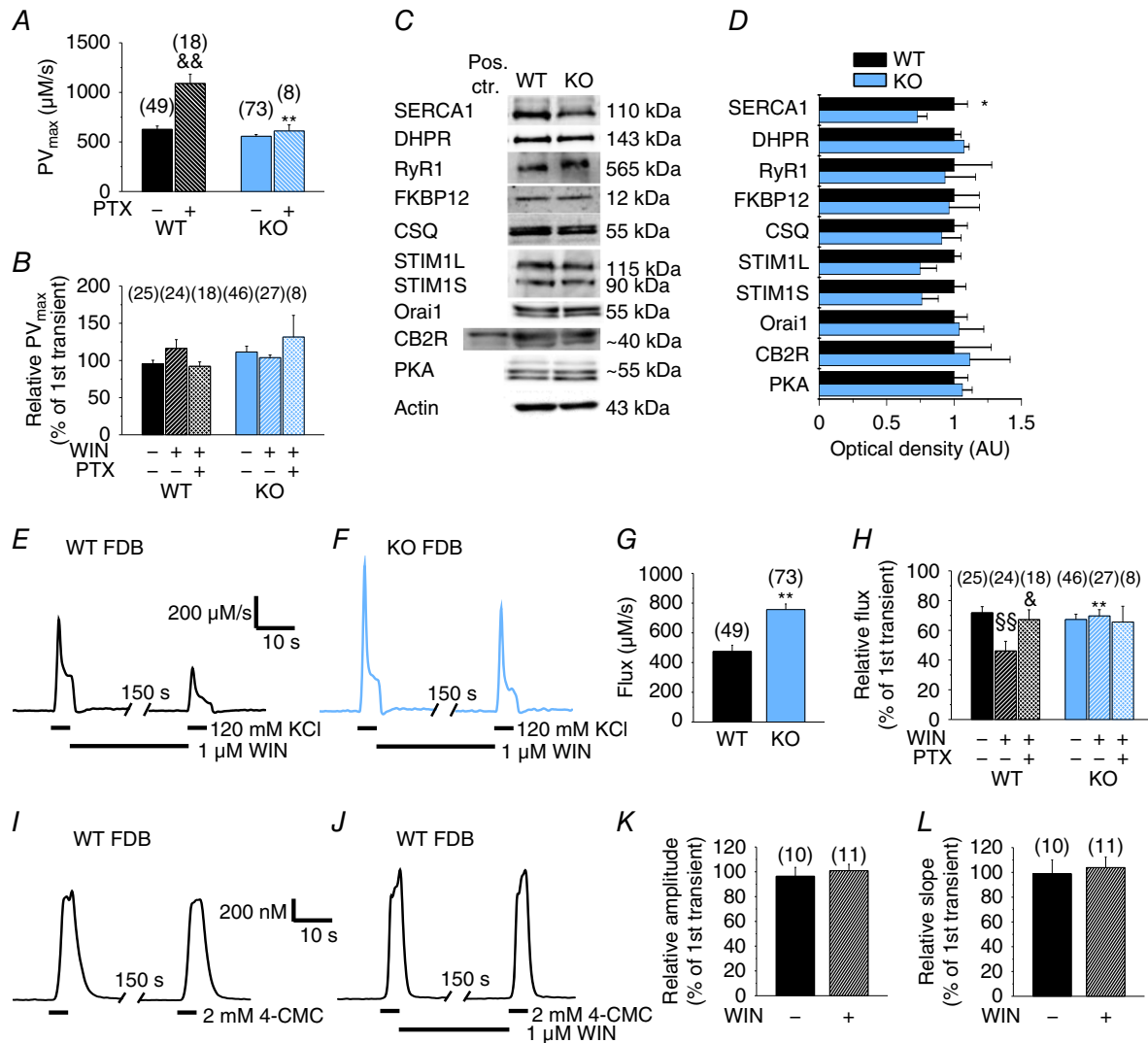


Figure 7. SERCA pump activity and calcium flux in WT, PTX-pre-treated ($1 \mu\text{g ml}^{-1}$, overnight) WT and KO FDB fibres

Pooled data of the calculated transport maximum of the SERCA pumps (A) and the same parameter of untreated and WIN-treated KCl-evoked second Ca^{2+} transients (B) normalized to that of the untreated first transients. C, representative images of western blot experiments showing the expression of proteins involved in the Ca^{2+} homeostasis of skeletal muscle. Whole hind limb muscle homogenates from at least three WT and three KO mice were used as samples. Spleen of a WT mouse was used as a positive control for CB2R. D, average optical density of the western blot bands normalized to actin and then to WT. Representative records of maximum calcium flux (the amount of calcium entering the cytosol in one second) of KCl-evoked Ca^{2+} transients before and after WIN-treatment in (E) WT and (F) KO FDB fibres. G, pooled data of maximum Ca^{2+} flux entering the cytoplasm via RyRs during the first KCl-depolarization of WT and KO FDB fibres. H, relative Ca^{2+} flux normalized to the first transient in untreated and WIN-treated FDB fibres. Repeated 4-CMC-evoked Ca^{2+} transients of WT FDB muscle fibres in the (I) absence and (J) presence of WIN. The relationship between the (K) amplitudes and the (L) slopes of the first and second transients expressed in percentage of the first transient. CSQ, calsequestrin; STIM1L/S, long/short isoform of stromal interaction molecule type 1. * $P < 0.05$ and ** $P < 0.01$, respectively, WT vs. KO mice. & $P < 0.05$ and && $P < 0.01$, respectively, PTX-treated vs. untreated WT fibres. §§ $P < 0.01$, WIN-treated vs. untreated fibres. [Colour figure can be viewed at wileyonlinelibrary.com]

not have any effect on the SERCA pump activity as assessed by comparing PV_{\max} values determined from Ca^{2+} transients measured before and after the application of the drug (Fig. 7B). A reduced protein expression of SERCA was observed in KO muscles (Fig. 7C and D), which was initially unexpected because PV_{\max} was similar to that in the control (Fig. 7A). The apparent contradiction can be reconciled in light of the effect of PTX on PV_{\max} , which indicates a primary increase in the activity of the individual pumps if the effect of CB1Rs is blocked, followed by a secondary, compensatory reduction in SERCA expression, negating the primary effect. In PTX-treated KO fibres, the PV_{\max} of SERCA was similar to that of the untreated KO fibres, and significantly lower than that observed in PTX-treated WT (Fig. 7A). These results suggest that KO fibres lack the constitutive activity of $G_{i/o}$ protein-mediated signalling present in the WT, indicating that CB1Rs are the only or the most dominant receptors in adult skeletal muscle with constitutive $G_{i/o}$ activity.

Other proteins involved in the Ca^{2+} homeostasis of the skeletal muscle, PKA and CB2Rs were also examined, although their expression did not change significantly in KO muscles (Fig. 7C and D).

Knowing the PV_{\max} values, the maximal Ca^{2+} flux via RyRs was determined (Fig. 7E and F). In KO fibres, this parameter was significantly ($P < 0.01$) higher than in WT fibres (Fig. 7G). In addition, in WT fibres, WIN treatment significantly ($P < 0.01$) reduced the flux of the second transients normalized to the first ones from $72 \pm 4\%$ ($n = 25$) to $46 \pm 7\%$ ($n = 24$) (Fig. 7H). In KO fibres, WIN treatment did not cause such differences ($67 \pm 4\%$, $n = 46$ in untreated; $70 \pm 4\%$, $n = 27$ in WIN-treated fibres; $P = 0.67$), indicating the CB1R-specificity of the effect (Fig. 7H). In WT but not in KO, pre-treatment with PTX rescued the effects of WIN ($P < 0.05$), increasing the normalized flux to a comparable value ($67 \pm 7\%$, $n = 18$) in untreated WT and KO fibres (Fig. 7H).

The effect of WIN on 4-CMC (the direct activator of RyR) evoked Ca^{2+} transients was tested in WT fibres (Fig. 7I and J). It did not alter the amplitude (Fig. 7K) and the maximal rate of rise (Fig. 7L) of the 4-CMC evoked transients, suggesting that it is not the agonist-mediated opening of RyR but, instead, its activation via coupling with DHPRs that is altered by the CB1R-mediated signalling.

Tetanic stimulation evokes higher Ca^{2+} transients with increased calcium release flux in KO fibres

To examine the CB1R-mediated effects on the Ca^{2+} transients under physiologically more relevant conditions, confocal line-scan images were recorded in Rhod-2-loaded, field-stimulated FDB fibres of WT (Fig. 8A and C) and KO (Fig. 8B and D) mice. In KO fibres, tetanic stimuli but not single pulses evoked

significantly ($P < 0.05$) higher Ca^{2+} transients (Fig. 8E), in agreement with the findings for the first transients by KCl depolarization (Fig. 6G). $[Ca^{2+}]_T$ (Fig. 8F–H) and the peak of the calcium release flux through the RyRs (Fig. 8I–K) (Bodnár *et al.* 2014) were similarly higher in KO fibres compared to WT ($P < 0.01$ and $P < 0.05$, respectively).

To test whether the direct pharmacological inhibition of PKA has similar effects to its CB1R-mediated, $G_{i/o}$ protein-dependent inhibition, $1 \mu M$ PKI was applied to WT fibres for 5 min between two consecutive single stimuli. Compared to control fibres, PKI significantly ($P < 0.01$) reduced the relative amplitude of the second transients (Fig. 8L) to a similar extent as that observed in WIN-treated fibres, supporting the involvement of the $G_{\alpha_{i/o}}$ subunits in the effect. Gallein ($20 \mu M$), an inhibitor of the $G\beta\gamma$ subunits, was also tested on WT fibres, although it did not alter significantly ($P = 0.3$) the amplitude of the transients (Fig. 8L), suggesting that the involvement of these subunits in the CB1R-mediated regulation of ECC is negligible.

Discussion

CB1R activation causes muscle fatigue

In the present study, we show for the first time that cannabinoid receptor-mediated signalling also participates in the regulation of ECC and Ca^{2+} homeostasis of mammalian skeletal muscle.

CB1R-KO mice performed significantly worse in all of our *in vivo* muscle performance tests. This was probably not a direct effect of the lack of CB1Rs in skeletal muscle; rather, it was a result of the lack of the receptor in the central nervous system causing depression (Valverde and Torrens 2012) and a reduction in the motivation of the mice to perform exercise. This idea was strengthened by the results of our *in vitro* force measurements, where no significant difference was observed in the twitch and tetanic force of KO, WT and WIN-treated muscles. Our observations also suggest that the neural background and not the direct effects on the muscles dominated in the medical marijuana-induced muscle weakness of some human patients (Lorente Fernandez *et al.* 2014) and the cannabinoid-induced hypoactivity of mice (Zimmer *et al.* 1999). This forms a contrast to isolated frog muscle fibre bundles, where cannabinoids had substantial direct effects on the muscles themselves (Huerta *et al.* 2009). For this contrast, the physiological differences between amphibian and mammalian muscles were probably responsible.

On the other hand, we found that the CB1R agonist-treated, isolated WT muscles were significantly more prone to fatigue. This suggests that CB1Rs of the muscles were also, to some extent, directly involved in the marijuana-induced fatigue reported by Renaud and Cormier (1986) in human patients. Cannabinoid-induced

fatigue can have several explanations. CB1R agonists were shown to decrease the formation of new mitochondria (Tedesco *et al.* 2010); however, this effect was probably not responsible for such a rapid change (~ 1 h). CB1R agonists can also decrease respiration in mitochondria by activating mitochondrial CB1Rs (Bénard *et al.* 2012),

therefore reducing the ATP production required for sustained muscle exercise. CB1R agonists also decrease the basal and the insulin-mediated glucose uptake (Lindborg *et al.* 2010), thus reducing the metabolic supply required for exercise. During our pCa–force measurements, a CB1R-mediated reduction in the Ca^{2+} sensitivity of the

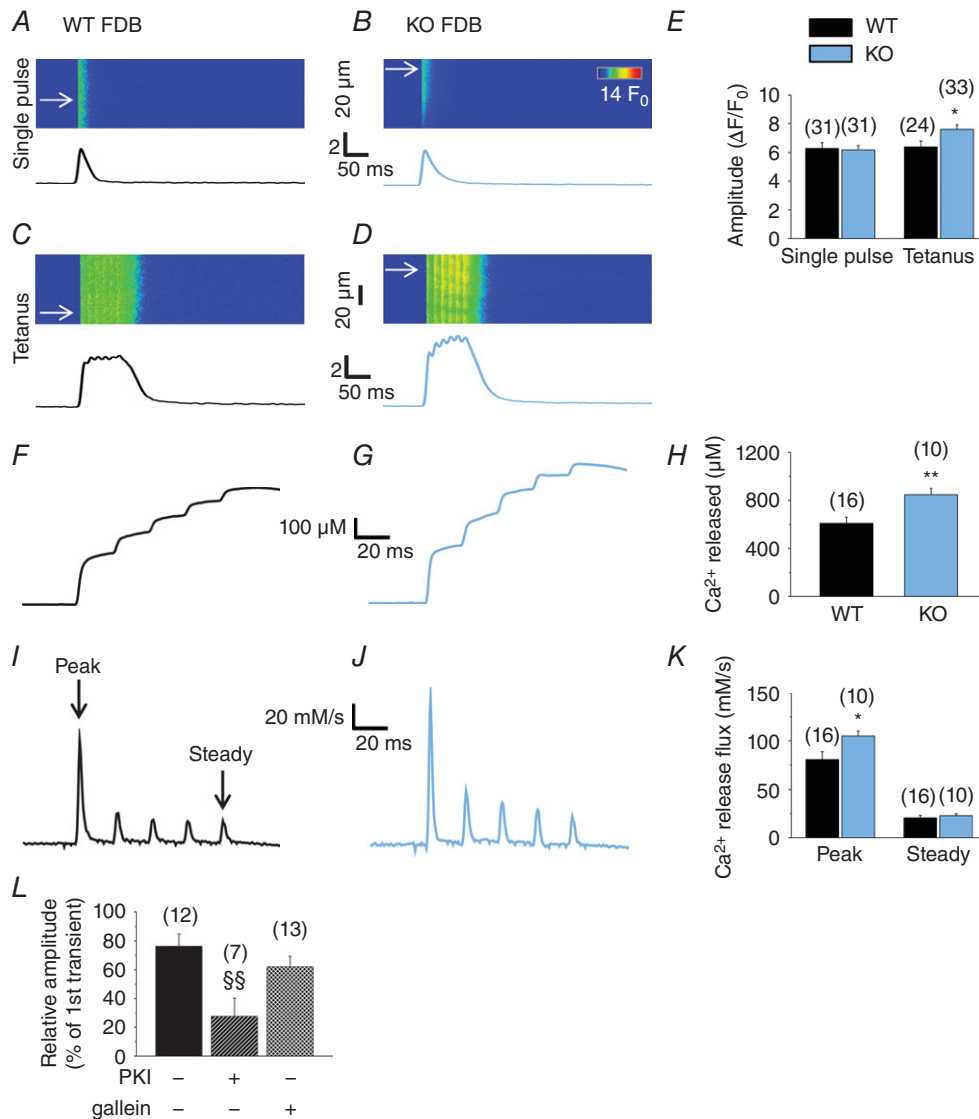


Figure 8. Tetanic electric stimulus evoked Ca^{2+} transients, Ca^{2+} release flux and the amount of released Ca^{2+} are higher in KO fibres

Confocal line-scan images were recorded on Rhod-2-loaded FDB fibres of WT and KO mice during field-stimulation. Representative records of Ca^{2+} transients evoked by a single stimulatory impulse (A in WT and B in KO FDB) or a tetanic stimulus (C in WT and D in KO FDB). Time courses were calculated from the average of eight to 20 lines indicated by arrows on the line-scan images. E, pooled data of the amplitude of the transients. Representative records of the total released amount of Ca^{2+} ($[\text{Ca}^{2+}]_{\text{T}}$) in (F) WT and (G) KO FDB fibres. H, pooled data of $[\text{Ca}^{2+}]_{\text{T}}$. I and J, corresponding calcium release flux through RyRs in WT and KO fibres, respectively. K, pooled data of the peak (first peak) and steady level (fifth peak) of the calcium release flux. L, two consecutive single stimuli were applied with a 5 min delay and, during the intermittent period, either PKI (1 μM) or gallein (20 μM) was applied to the fibres. Relative amplitude of the second transients, expressed as a percentage of the first transient on the same fibre before the treatment. Numbers in parentheses show the number of FDB fibres examined. * $P < 0.05$ and ** $P < 0.01$, respectively, WT vs. KO mice. §§ $P < 0.01$, PKI- or gallein-treated WT vs. untreated. [Colour figure can be viewed at wileyonlinelibrary.com]

contractile proteins was also observed, such that a higher $[Ca^{2+}]_i$ was needed to achieve the same contractile force in WIN-treated fibres, which might not be able to fully explain but could contribute to the increased fatigability, especially because, as demonstrated subsequently, Ca^{2+} release was also compromised. Thus, we next examined in detail the role of CB1R-mediated pathways in the Ca^{2+} homeostasis of the developing myotubes and adult fibres.

CB1 signalling in skeletal muscle does not affect the IP_3 pathway

Activation of CB1Rs was suggested to activate G_q proteins and to release Ca^{2+} from the intracellular stores via IP_3 receptors in a number of different cell types, including astrocytes (Navarrete and Araque 2008), dorsal root ganglion neurons (Liu *et al.* 2009), insulinoma cells (De Petrocellis *et al.* 2007) and CB1R-expressing HEK293 cells (Lauckner *et al.* 2005). In CB1R-expressing CHO cells, the connection of CB1Rs to G_q proteins and phosphatidylinositol 4,5-bisphosphate depletion was also demonstrated, and the same was also proposed for cultured skeletal muscle cells (Iannotti *et al.* 2014). We tested the highly specific CB1R agonist ACEA and the general CB1R and CB2R agonist WIN on C2C12 myotubes and on adult FDB fibres. Although members of the IP_3 pathway are present on skeletal muscle (Jaimovich *et al.* 2000), none of these drugs could evoke Ca^{2+} transients, showing that, in skeletal muscle, in contrast to heterologous expression systems, as well as neural or epithelial cells, CB1Rs are not connected to G_q proteins; rather (as is discussed below) they are connected to $G_{i/o}$ proteins as suggested by Huerta *et al.* (2009) and do not induce a release of Ca^{2+} via IP_3 receptors. Additionally, by examining the effects of CB1R activation on the P2Y metabotropic purinergic receptor-mediated Ca^{2+} transients, we could conclude that the CB1R-mediated signalling does not even regulate the IP_3 -mediated Ca^{2+} release in myotubes.

CB1R attenuates ECC via $G_{i/o}$ proteins

By ruling out coupling to G_q proteins, we assumed that CB1Rs couple to $G_{i/o}$ proteins and decrease the activity of adenylyl cyclase and PKA. This then reduces the extent of phosphorylation of different proteins, presumably including DHPR (Hulme *et al.* 2005; Fuller *et al.* 2014), RyR (Igami *et al.* 1999; Ozawa 2010) and regulatory proteins of SERCA (Morita *et al.* 2008), with all of them playing important roles in ECC. To confirm this hypothesis, the effects of the absence and the activation of CB1Rs were studied on depolarization-evoked Ca^{2+} transients.

Interestingly, in C2C12 myotubes, we could not detect any effects of CB1R activation, indicating that some

components of the CB1R-mediated signalling pathway are not yet present or functional on these cells. Alternatively, at this stage of muscle development, CB1R activation may only affect myogenesis (Iannotti *et al.* 2014), without influencing the Ca^{2+} signalling mechanisms.

On the other hand, in adult KO skeletal muscle fibres, the absence of CB1Rs significantly increased the amplitude of the depolarization-induced Ca^{2+} transients, the total amount of Ca^{2+} released during tetanic stimulation and the Ca^{2+} release flux through RyR. These indicate that RyR is one of the possible main downstream targets of the CB1R-mediated signalling, and also suggest the presence of a continuous negative control on these Ca^{2+} release channels mediated by a CB1R-dependent pathway in WT muscles. The above mentioned inhibitory effect was further amplified by activation of CB1Rs by WIN or AEA in WT but not in KO fibres, confirming the CB1R-specificity of this phenomenon.

Initially, there appears to be a contradiction between the higher Ca^{2+} but similar force transients in KO muscles compared to WT. However, in the case of tetani, we can assume that the relatively smaller amplitude of the Ca^{2+} transients in WT (even in WIN-treated WT) is already capable of fully activating the contractile system. In this framework two conclusions follow. First, in a normal (WT) muscle, the tetanic stimulation fully activates the contractile machinery (there is no need to have any reserve; this is achieved by not activating all fibres in the given muscle); therefore, larger force transients are not expected even if $[Ca^{2+}]_i$ is greater. Second, any further increase in released Ca^{2+} is a 'waste' and does not generate larger force. In this respect, CB1R-mediated signalling helps muscles to be more 'efficient'. One could take this speculation even further by stating that if, for any reason, the function of the contractile machinery is altered, there is a reserve in the system ('turning off' the constitutive activity of the cannabinoid signalling) to improve/increase force.

The effect of the CB1R agonist treatment was reversible by inhibiting $G_{i/o}$ proteins with pertussis toxin, confirming the involvement of these G proteins in CB1R-mediated signalling. Moreover, the direct pharmacological inhibition of PKA resulted in a similar effect (i.e. a marked reduction of the Ca^{2+} transients), strengthening the conclusions drawn from our previous experiments. Thus, it can be proposed that, in adult skeletal muscle fibres, the agonist-mediated or constitutive (Nie and Lewis 2001) activity of CB1R activates $G_{i/o}$ proteins, which decreases the level of cAMP, the activity of PKA and the phosphorylation of RyR (Igami *et al.* 1999; Ozawa 2010) or other proteins involved in ECC (e.g. the DHPR), thereby decreasing the magnitude of the RyR-mediated Ca^{2+} current (Fig. 9). However, an indirect regulatory effect of the CB1R-mediated signalling on SR Ca^{2+} release, where the recovery from inactivation of the

above mentioned receptors is affected, cannot be ruled out either.

Although several research groups have demonstrated that cannabinoids inhibit other (N, P, P/Q and T) types of Ca^{2+} channels, as reviewed by Pertwee *et al.* (2010), and Zhuang *et al.* (2005) have described the regulatory effect of these drugs on RyRs in hippocampal neurons, to our knowledge, the present study is the first to demonstrate any role of the cannabinoid system in the RyR-mediated Ca^{2+} release and ECC in muscle. In skeletal muscle, the localization of CB1Rs around the Z-lines, between the T-tubules of the muscle fibres also supports the idea of an effective, spatially co-ordinated regulatory apparatus with the involvement of both receptors. If RyRs are regulated by CB1Rs similarly in amphibians, our results can explain those previous observations where

CB1R-agonist treatment caused the weaker contractile force of frog muscles (Huerta *et al.* 2009). Moreover, they resemble the results obtained for smooth (Baldassano *et al.* 2008; Makwana *et al.* 2010; Grassin-Delyle *et al.* 2014; Sánchez-Pastor *et al.* 2014) and cardiac (Bonz *et al.* 2003; Li *et al.* 2009) muscle, where CB1R agonists similarly attenuated and the antagonists enhanced muscle contractions and Ca^{2+} transients, although RyRs were not mentioned among the downstream targets of cannabinoid signalling in any of these studies.

Our experiments with 4-CMC, the direct activator of RyR, suggest that the DHPR-RyR interaction is affected by the cannabinoid signalling and not the Ca^{2+} release via agonist-mediated opening of RyR. However, these experiments do not discriminate whether the CB1R-mediated effects take place at the RyR or DHPR side in ECC. Thus, we cannot rule out the effects of PKA-phosphorylation of DHPRs with respect to the increased Ca^{2+} transients of the KO fibres. PKA is anchored by an A-kinase anchoring protein to the autoinhibitory distal C-terminus of the skeletal and cardiac voltage-gated Ca^{2+} channels (CaV1). Protein phosphorylation by PKA increases ion conductance activity by relieving the autoinhibitory effect of the distal C terminus (Hulme *et al.* 2005, Fuller *et al.* 2014), although it is not known how it affects the voltage sensitivity of DHPR or its conformation change by which RyR is activated during ECC.

It is also conceivable that the effects observed upon CB1R stimulation were not only caused by the activation of the α subunits of the G proteins, but also were mediated to some extent by their $G\beta\gamma$ subunits. Activation of G protein-coupled receptors following extracellular agonist stimulation results in the activation of two intracellular signalling molecules, $G\alpha$ -GTP (its presumable effects were discussed above in detail) and the free $G\beta\gamma$ dimer. $G\beta\gamma$ -mediated regulation generally occurs through direct binding of the dimer to target effectors. In neurons, the $G\beta\gamma$ dimer is known to inhibit CaV through its direct binding to the CaV2 α subunit (De Waard *et al.* 2005). A relatively recent study in adult mammalian skeletal muscle has shown that the expression of $G\beta 1\gamma 2$ dimer inhibits the CaV1.1 (DHPR) Ca^{2+} current and the voltage-activated SR Ca^{2+} release process (Weiss *et al.* 2010). Thus, it is possible that the observed regulatory effects on ECC did not exclusively arise from CB1R-dependent activation of $G\alpha_{i/o}$ but, instead, were a result of CB1R-dependent regulation of CaV1.1 (or indirect regulation of RyR1) mediated by $G\beta\gamma$ subunits. In support of this view, CB1R activation is associated with $G\beta\gamma$ -dependent activation of different effectors, including ion channels, the kinases phosphoinositide 3-kinase, Src and mitogen-activated protein kinase cascades (Keimpema *et al.* 2011). In addition, CB1R signals also through non-G protein partners such as the adaptor protein FAN (factor

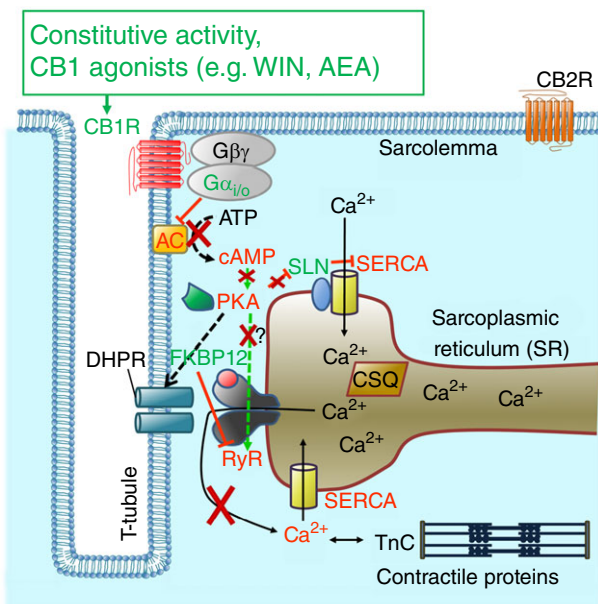


Figure 9. The proposed mechanism how CB1 receptors regulate ECC in skeletal muscle

Depolarization of the membrane activates DHPRs, which directly open RyRs and release Ca^{2+} from the SR, activating the contractile apparatus of the muscle fibre. The Ca^{2+} is re-uptaken by the SERCA pumps to the SR. SERCA is regulated by SLN: PKA-mediated phosphorylation of SLN increases the pump activity. A constitutive or agonist-mediated activation of CB1Rs activates $G\alpha_{i/o}$ proteins and decreases the activity of AC, thus reducing the concentration of cAMP, inactivating PKA. Two mechanisms are possible: (1) RyR remains dephosphorylated and binds FKBP12, which decreases the open probability of RyR, allowing less Ca^{2+} release from the SR. (2) Decreased phosphorylation of DHPR or RyR disrupts their interaction, resulting in a smaller Ca^{2+} release. SLN also remains dephosphorylated and attenuates Ca^{2+} uptake via SERCA. The contribution of the $\beta\gamma$ subunits of the G-proteins to this process appears to be negligible. Colour code: red indicates inactivation, whereas green indicates activation of a protein as a consequence of CB1R activation. AC, adenylyl cyclase; CSQ, calsequestrin; TnC, troponin-C.

associated with neutral sphingomyelinase activation). However, inhibition of the $G\beta\gamma$ subunits did not alter the amplitude of the Ca^{2+} transients significantly, suggesting that the role of these subunits in the CB1R-mediated regulation of ECC is negligible in skeletal muscle.

CB1R attenuates SERCA activity

A CB1R-mediated decrease in the PKA activity may also affect the regulatory proteins of the SERCA pump: phospholamban (PLB) in slow skeletal muscle and heart (Liu *et al.* 1997) and sarcolipin (SLN) in fast skeletal muscle (Odermatt *et al.* 1998). PKA-mediated phosphorylation of PLB and SLN leads to their conformational change, as well as to a higher Ca^{2+} uptake rate of SERCA (Morita *et al.* 2008); thus, CB1R activation was expected to reduce SERCA activity.

Consistent with this, in PTX-treated WT fibres, as a result of the enhanced PKA activity, a markedly increased Ca^{2+} transport rate was observed. In KO fibres, where we also expected a higher PKA and SERCA activity as a result of the missing constitutive inhibitory action of CB1Rs and the coupling $G_{i/o}$ proteins, the PV_{max} was surprisingly similar to that of the untreated WT. Taking into consideration the significantly reduced SERCA expression of KO muscles, and because the total PV_{max} was found to be similar to that of WT, the individual pump activity had to be significantly higher in KO fibres. This means that the increased pump activity in KO fibres was masked by a compensatory reduction in the SERCA protein expression. Thus, similar to the case of RyR, we can assume a continuous negative regulatory effect of the CB1R-mediated signalling on SERCA activity in WT fibres, which was missing in KO fibres.

On the other hand, SERCA activity was not affected by WIN treatment, suggesting that PLB/SLN are normally dephosphorylated in WT fibres, and their phosphorylation state could not be decreased further by the activation of the CB1R-mediated signalling.

It is worth noting that the expression of the main Ca^{2+} binding protein of the SR Ca^{2+} store (i.e. calsequestrin) was mostly unchanged in KO muscles. Similarly, the expression of STIM1, the Ca^{2+} sensor of the SR, and key activator molecule of the store-operated Ca^{2+} entry mechanism, and Orai1, the main store-operated Ca^{2+} channel (Pan *et al.* 2014), was also unaltered in KO muscles. According to the PhosphoSitePlus® database (Hornbeck *et al.* 2015), these proteins are not phosphorylated by PKA. These observations suggest that CB1R-mediated signalling most probably does not interfere with Ca^{2+} storage functions of the SR. In CB2R expression, we also did not find any difference between WT and KO muscle samples, ruling out the possibility that the lack of CB1R upregulates this other cannabinoid signalling pathway.

Conclusions

In summary, the present study provides answers to previously unresolved questions; namely, which signal transduction pathway is connected to CB1Rs in mammalian skeletal muscle and how the absence or activation of the receptors affects ECC and muscle force. The results confirm that CB1R-mediated signalling in skeletal muscle inhibits the RyR-mediated Ca^{2+} transients via a $G_{i/o}$ protein and PKA-dependent way, alters the activity of SERCA, reduces the Ca^{2+} -sensitivity of the contractile proteins and increases muscle fatigue.

These results, together with those previously obtained by other research groups, with respect to studies investigating the decrease of myogenesis and myoblast differentiation (Iannotti *et al.* 2014), the reduction of the glucose uptake of the muscles (Lindborg *et al.* 2010), the reduction of the mitochondrial biogenesis (Tedesco *et al.* 2010) and ATP production (Bénard *et al.* 2012, Fišar *et al.* 2014), and the neuronal effects decreasing the locomotor activity (Zimmer *et al.* 1999), indicate a complex, systemic inhibitory role of the cannabinoid system on muscle activity. However the same observations raise the possibility that antagonists of CB1Rs could be used as potent stimulators of muscle force and regeneration during ageing and in muscle-wasting diseases. These results can contribute to the understanding of the role of the endocannabinoid system in myopathies and the development of new cannabinoid drugs by identifying their muscle-specific action or side-effects, and also draw attention to the risks of marijuana smoking on physical performance.

References

- Baldassano S, Serio R & Mule' F (2008). Cannabinoid CB(1) receptor activation modulates spontaneous contractile activity in mouse ileal longitudinal muscle. *Eur J Pharmacol* **582**, 132–138.
- Bénard G, Massa F, Puente N, Lourenço J, Bellocchio, L, Soria-Gómez E, Matias I, Delamarre A, Metna-Laurent M, Cannich A, Hebert-Chatelain E, Mülle C, Ortega-Gutiérrez S, Martín-Fontecha M, Klugmann M, Guggenhuber S, Lutz B, Gertsch J, Chaoulhoff F, López-Rodríguez ML, Grandes P, Rossignol R & Marsicano G (2012). Mitochondrial CB₁ receptors regulate neuronal energy metabolism. *Nat Neurosci* **15**, 558–564.
- Bodnár D, Geyer N, Ruzsnavszky O, Oláh T, Hegyi B, Sztretye M, Fodor J, Dienes B, Balogh Á, Papp Z, Szabó L, Müller G, Csernoch L & Szentesi P (2014). Hypermuscular mice with mutation in the myostatin gene display altered calcium signalling. *J Physiol* **592**, 1353–1365.
- Bonz A, Laser M, Küllmer S, Kniesch S, Babin-Ebell J, Popp V, Ertl G & Wagner JA (2003). Cannabinoids acting on CB1 receptors decrease contractile performance in human atrial muscle. *J Cardiovasc Pharmacol* **41**, 657–664.

- Borgelt LM, Franson KL, Nussbaum AM & Wang GS (2013). The pharmacologic and clinical effects of medical cannabis. *Pharmacotherapy* **33**, 195–209.
- Buckman JF, Yusko DA, Farris SG, White HR & Pandina RJ (2011). Risk of marijuana use in male and female college student athletes and nonathletes. *J Stud Alcohol Drugs* **72**, 586–591.
- Burnstock G, Arnett TR & Orriss IR (2013). Purinergic signalling in the musculoskeletal system. *Purinergic Signal* **9**, 541–572.
- Cavuoto P, McAinch AJ, Hatzinikolas G, Janovská A, Game P & Wittert GA (2007). The expression of receptors for endocannabinoids in human and rodent skeletal muscle. *Biochem Biophys Res Commun* **364**, 105–110.
- Crespillo A, Suárez J, Bermúdez-Silva FJ, Rivera P, Vida M, Alonso M, Palomino A, Lucena MA, Serrano A, Pérez-Martín M, Macías M, Fernández-Llébraz P & Rodríguez de Fonseca F (2011). Expression of the cannabinoid system in muscle: effects of a high-fat diet and CB1 receptor blockade. *Biochem J* **433**, 175–185.
- De Petrocellis L, Marini P, Matias I, Moriello AS, Starowicz K, Cristino L, Nigam S & Di Marzo V (2007). Mechanisms for the coupling of cannabinoid receptors to intracellular calcium mobilization in rat insulinoma beta-cells. *Exp Cell Res* **313**, 2993–3004.
- De Waard M, Hering J, Weiss N & Feltz A (2005). How do G proteins directly control neuronal Ca²⁺ channel function? *Trends Pharmacol Sci* **26**, 427–436.
- Devane WA, Hanus L, Breuer A, Pertwee RG, Stevenson LA, Griffin G, Gibson D, Mandelbaum A, Etinger A & Mechoulam R (1992). Isolation and structure of a brain constituent that binds to the cannabinoid receptor. *Science* **258**, 1946–1949.
- Esposito I, Proto MC, Gazerro P, Laezza C, Miele C, Alberobello AT, D'Esposito V, Beguinot F, Formisano P & Bifulco M (2008). The cannabinoid CB1 receptor antagonist rimonabant stimulates 2-deoxyglucose uptake in skeletal muscle cells by regulating the expression of phosphatidylinositol-3-kinase. *Mol Pharmacol* **74**, 1678–1686.
- Fišar Z, Singh N & Hroudová J (2014). Cannabinoid-induced changes in respiration of brain mitochondria. *Toxicol Lett* **231**, 62–71.
- Franzini-Armstrong C & Protasi F (1997). Ryanodine receptors of striated muscles: a complex channel capable of multiple interactions. *Physiol Rev* **77**, 699–729.
- Friedrich O, Yi B, Edwards JN, Reischl B, Wirth-Hücking A, Buttgerit A, Lang R, Weber C, Polyak F, Liu I, von Wegner F, Cully TR, Lee A, Most P & Völkens M (2014). IL-1 α reversibly inhibits skeletal muscle ryanodine receptor: a novel mechanism for critical illness myopathy? *Am J Respir Cell Mol Biol* **50**, 1096–1106.
- Fuller MD, Fu Y, Scheuer T & Catterall WA (2014). Differential regulation of CaV1.2 channels by cAMP-dependent protein kinase bound to A-kinase anchoring proteins 15 and 79/150. *J Gen Physiol* **143**, 315–324.
- Grassin-Delyle S, Naline E, Buenestado A, Faisy C, Alvarez JC, Salvator H, Abrial C, Advenier C, Zemoura L & Devillier P (2014). Cannabinoids inhibit cholinergic contraction in human airways through prejunctional CB1 receptors. *Br J Pharmacol* **171**, 2767–2777.
- Hornbeck PV, Zhang B, Murray B, Kornhauser JM, Latham V & Skrzypek E (2015). PhosphoSitePlus, 2014: mutations, PTMs and recalibrations. *Nucleic Acids Res* **43**, D512–D520.
- Huerta M, Ortiz-Mesina M, Trujillo X, Sánchez-Pastor E, Vásquez C, Castro E, Velasco R, Montoya-Pérez R & Onetti C (2009). Effects of cannabinoids on caffeine contractures in slow and fast skeletal muscle fibers of the frog. *J Membr Biol* **229**, 91–99.
- Hulme JT, Konoki K, Lin TW, Gritsenko MA, Camp DG 2nd, Bigelow DJ & Catterall WA (2005). Sites of proteolytic processing and noncovalent association of the distal C-terminal domain of CaV1.1 channels in skeletal muscle. *Proc Natl Acad Sci USA* **102**, 5274–5279.
- Hutchins-Wiese HL, Li Y, Hannon K & Watkins BA (2012). Hind limb suspension and long-chain omega-3 PUFA increase mRNA endocannabinoid system levels in skeletal muscle. *J Nutr Biochem* **23**, 986–993.
- Iannotti FA, Silvestri C, Mazzarella E, Martella A, Calvigioni D, Piscitelli F, Ambrosino P, Petrosino S, Cifra G, Bíró T, Harkany T, Tagliamonte M & Di Marzo V (2014). The endocannabinoid 2-AG controls skeletal muscle cell differentiation via CB1 receptor-dependent inhibition of Kv7 channels. *Proc Natl Acad Sci USA* **111**, E2472–E2481.
- Igami K, Yamaguchi N & Kasai M (1999). Regulation of depolarization-induced calcium release from skeletal muscle triads by cyclic AMP-dependent protein kinase. *Jpn J Physiol* **49**, 81–87.
- Jaimovich E, Reyes R, Liberona JL & Powell JA (2000). IP(3) receptors, IP(3) transients, and nucleus-associated Ca(2+) signals in cultured skeletal muscle. *Am J Physiol Cell Physiol* **278**, C998–C1010.
- Keimpema E, Mackie K & Harkany T (2011). Molecular model of cannabis sensitivity in developing neuronal circuits. *Trends Pharmacol Sci* **32**, 551–561.
- Lauckner JE, Hille B & Mackie K (2005). The cannabinoid agonist WIN55,212-2 increases intracellular calcium via CB1 receptor coupling to Gq/11 G proteins. *Proc Natl Acad Sci USA* **102**, 19144–19149.
- Li Q, Ma HJ, Zhang H, Qi Z, Guan Y & Zhang Y (2009). Electrophysiological effects of anandamide on rat myocardium. *Br J Pharmacol* **158**, 2022–2029.
- Lindborg KA, Teachey MK, Jacob S & Henriksen EJ (2010). Effects of in vitro antagonism of endocannabinoid-1 receptors on the glucose transport system in normal and insulin-resistant rat skeletal muscle. *Diabetes Obes Metab* **12**, 722–730.
- Lipina C, Stretton C, Hastings S, Hundal JS, Mackie K, Irving AJ & Hundal HS (2010). Regulation of MAP kinase-directed mitogenic and protein kinase B-mediated signaling by cannabinoid receptor type 1 in skeletal muscle cells. *Diabetes* **59**, 375–385.

- Liu Q, Bhat M, Bowen WD & Cheng J (2009). Signaling pathways from cannabinoid receptor-1 activation to inhibition of N-methyl-D-aspartic acid mediated calcium influx and neurotoxicity in dorsal root ganglion neurons. *J Pharmacol Exp Ther* **331**, 1062–1070.
- Liu Y, Kranias EG & Schneider MF (1997). Regulation of Ca²⁺ handling by phosphorylation status in mouse fast- and slow-twitch skeletal muscle fibers. *Am J Physiol Cell Physiol* **273**, C1915–C1924.
- Lorente Fernández L, Monte Boquet E, Pérez-Miralles F, Gil Gómez I, Escutia Roig M, Boscá Blasco I, Poveda Andrés JL & Casanova-Estruch B (2014). Clinical experiences with cannabinoids in spasticity management in multiple sclerosis. *Neurología* **29**, 257–260.
- Maccarrone M, Bab I, Bíró T, Cabral GA, Dey SK, Di Marzo V, Konje JC, Kunos G, Mechoulam R, Pacher P, Sharkey KA & Zimmer A (2015). Endocannabinoid signaling at the periphery: 50 years after THC. *Trends Pharmacol Sci* **36**, 277–296.
- Makwana R, Molleman A & Parsons ME (2010). Evidence for both inverse agonism at the cannabinoid CB1 receptor and the lack of an endogenous cannabinoid tone in the rat and guinea-pig isolated ileum myenteric plexus-longitudinal muscle preparation. *Br J Pharmacol* **160**, 615–626.
- Morita T, Hussain D, Asahi M, Tsuda T, Kurzydowski K, Toyoshima C & MacLennan DH (2008). Interaction sites among phospholamban, sarcolipin, and the sarco(endo)plasmic reticulum Ca(2+)-ATPase. *Biochem Biophys Res Commun* **369**, 188–194.
- Navarrete M & Araque A (2008). Endocannabinoids mediate neuron-astrocyte communication. *Neuron* **57**, 883–893.
- Nie J & Lewis DL (2001). Structural domains of the CB1 cannabinoid receptor that contribute to constitutive activity and G-protein sequestration. *J Neurosci.* **21**, 8758–8774.
- Oddoux S, Brocard J, Schweitzer A, Szentesi P, Giannesini B, Brocard J, Fauré J, Pernet-Gallay K, Bendahan D, Lunardi J, Csernoch L & Marty I (2009). Triadin deletion induces impaired skeletal muscle function. *J Biol Chem* **284**, 34918–34929.
- Odermatt A, Becker S, Khanna VK, Kurzydowski K, Leisner E, Pette D & MacLennan DH (1998). Sarcolipin regulates the activity of SERCA1, the fast-twitch skeletal muscle sarcoplasmic reticulum Ca²⁺-ATPase. *J Biol Chem* **273**, 12360–12369.
- Oláh T, Fodor J, Ruzsnavszky O, Vincze J, Berbey C, Allard B & Csernoch L (2011). Overexpression of transient receptor potential canonical type 1 (TRPC1) alters both store operated calcium entry and depolarization-evoked calcium signals in C2C12 cells. *Cell Calcium* **49**, 415–425.
- Ozawa T (2010). Modulation of ryanodine receptor Ca²⁺ channels. *Mol Med Rep* **3**, 199–204.
- Pacher P & Kunos G (2013). Modulating the endocannabinoid system in human health and disease – successes and failures. *FEBS J* **280**, 1918–1943.
- Pan Z, Brotto M & Ma J (2014). Store-operated Ca²⁺ entry in muscle physiology and diseases. *BMB Rep* **47**, 69–79.
- Pertwee RG, Howlett AC, Abood ME, Alexander SP, Di Marzo V, Elphick MR, Greasley PJ, Hansen HS, Kunos G, Mackie K, Mechoulam R & Ross RA (2010). International Union of Basic and Clinical Pharmacology. LXXIX. Cannabinoid receptors and their ligands: beyond CB₁ and CB₂. *Pharmacol Rev* **62**, 588–631.
- Renaud AM & Cormier Y (1986). Acute effects of marijuana smoking on maximal exercise performance. *Med Sci Sports Exerc* **18**, 685–689.
- Rowland LA, Bal NC & Periasamy M (2015). The role of skeletal-muscle-based thermogenic mechanisms in vertebrate endotherm. *Biol Rev Camb Philos Soc* **90**, 1279–1297.
- Sánchez-Pastor E, Andrade F, Sánchez-Pastor JM, Elizalde A, Huerta M, Virgen-Ortiz A, Trujillo X & Rodríguez-Hernández A (2014). Cannabinoid receptor type 1 activation by arachidonylcyclopropylamide in rat aortic rings causes vasorelaxation involving calcium-activated potassium channel subunit alpha-1 and calcium channel, voltage-dependent, L type, alpha 1C subunit. *Eur J Pharmacol* **729**, 100–106.
- Sinacore DR & Gulve EA (1993). The role of skeletal muscle in glucose transport, glucose homeostasis, and insulin resistance: implications for physical therapy. *Phys Ther.* **73**, 878–891.
- Stammers AN, Susser SE, Hamm NC, Hlynsky MW, Kimber DE, Kehler DS & Duhamel TA (2015). The regulation of sarco(endo)plasmic reticulum calcium-ATPases (SERCA). *Can J Physiol Pharmacol.* **93**, 843–854.
- Szappanos H, Cseri J, Deli T, Kovács L & Csernoch L (2004). Determination of depolarisation- and agonist-evoked calcium fluxes on skeletal muscle cells in primary culture. *J Biochem Biophys Methods* **59**, 89–101.
- Taube A, Eckardt K & Eckel J (2009). Role of lipid-derived mediators in skeletal muscle insulin resistance. *Am J Physiol Endocrinol Metab* **297**, E1004–E1012.
- Tedesco L, Valerio A, Dossena M, Cardile A, Ragni M, Pagano C, Pagotto U, Carruba MO, Vettor R & Nisoli E (2010). Cannabinoid receptor stimulation impairs mitochondrial biogenesis in mouse white adipose tissue, muscle, and liver: the role of eNOS, p38 MAPK, and AMPK pathways. *Diabetes* **59**, 2826–2836.
- Turu G & Hunyady L (2010). Signal transduction of the CB1 cannabinoid receptor. *J Mol Endocrinol* **44**, 75–85.
- Valverde O & Torrens M (2012). CB1 receptor-deficient mice as a model for depression. *Neuroscience* **204**, 193–206.
- Weiss N, Legrand C, Pouvreau S, Bichraoui H, Allard B, Zamponi GW, De Waard M & Jacquemond V (2010). In vivo expression of G-protein beta1gamma2 dimer in adult mouse skeletal muscle alters L-type calcium current and excitation-contraction coupling. *J Physiol* **588**, 2945–2960.
- Zhuang SY, Bridges D, Grigorenko E, McCloud S, Boon A, Hampson RE & Deadwyler SA (2005). Cannabinoids produce neuroprotection by reducing intracellular calcium release from ryanodine-sensitive stores. *Neuropharmacology* **48**, 1086–1096.

Zimmer A, Zimmer AM, Hohmann AG, Herkenham M & Bonner TI (1999). Increased mortality, hypoactivity, and hypoalgesia in cannabinoid CB1 receptor knockout mice. *Proc Natl Acad Sci USA* **96**, 5780–5785.

Additional information

Competing interests

The authors declare that they have no competing interests.

Author contributions

TO, DB, JV, AT, JF, BR, AK, OR, BD and PSz performed the experiments, and also collected, analysed and interpreted data. TO, OF and LCs designed and supervised the study, analysed and interpreted data, and wrote the paper. All authors approved the final version of the manuscript. All persons designated as authors qualify for authorship, and all those who qualify for authorship are listed. Measurements of muscle force in small fibre

bundles were performed at the Friedrich-Alexander-University Erlangen-Nürnberg. All other experiments were performed at the University of Debrecen.

Funding

TO and JV were supported by the European Union and the State of Hungary, co-financed by the European Social Fund in the framework of TÁMOP 4.2.4. A/2-11-1-2012-0001 'National Excellence Program'. The work was supported by research grants from the Hungarian Scientific Research Fund (OTKA K-115461) and TÁMOP-4.1.2.E-13/1/KONV-2013-0010.

Acknowledgements

The authors are indebted to Róza Óri and Sabine Lessig for their excellent technical assistance, as well as Csilla Bordás, Biborka Nádró and Anna Farkas for their help with the *in vivo* tests and genotyping. CB1R-KO mice were a kind gift from Dr Andreas Zimmer.